Journal of Innovative Optical Health Sciences
Vol. 13, No. 3 (2020) 2030005 (11 pages)

DOI: 10.1142/S1793545820300050

Photoacoustic reporter genes for noninvasive molecular imaging and theranostics

Zhao Lei*, Yun Zeng†, Xiaofen Zhang*, Xiaoyong Wang*,‡ and Gang Liu*,§
*State Key Laboratory of Molecular Vaccinology and Molecular Diagnostics & Center for Molecular Imaging and Translational Medicine
School of Public Health
Xiamen University, Xiamen 361102, P. R. China
†Department of Pharmacy, Xiamen Medical College
Xiamen, Fujian 361023, P. R. China
‡wangxy@xmu.edu.cn
§gangliu.cmitm@xmu.edu.cn

Received 4 November 2019
Accepted 14 December 2019
Published 31 January 2020

Noninvasive molecular imaging makes the observation and comprehensive understanding of complex biological processes possible. Photoacoustic imaging (PAI) is a fast evolving hybrid imaging technology enabling *in vivo* imaging with high sensitivity and spatial resolution in deep tissue. Among the various probes developed for PAI, genetically encoded reporters attracted increasing attention of researchers, which provide improved performance by acquiring images of a PAI reporter gene's expression driven by disease-specific enhancers/promoters. Here, we present a brief overview of recent studies about the existing photoacoustic reporter genes (RGs) for noninvasive molecular imaging, such as the pigment enzyme reporters, fluorescent proteins and chromoproteins, photoswitchable proteins, including their properties and potential applications in theranostics. Furthermore, the challenges that PAI RGs face when applied to the clinical studies are also examined.

Keywords: Photoacoustic imaging; reporter genes; noninvasive molecular imaging; genetically encoded probe; theranostic application.

1. Introduction

As a rapidly evolving biomedical discipline, molecular imaging provides noninvasive visual quantitative representations of biological processes in living organisms.[1] With the combination of molecular biotechnology and radiological imaging,

‡,§Corresponding authors.

noninvasive molecular-imaging technologies have outstanding advantages in characterizing diseased tissues without surgical procedures or invasive biopsies, therefore offering the researchers and clinicians exciting new opportunities in screening and early diagnosis, disease-specific treatment and personalized theranostics.[2,3] Current clinical molecular imaging methods include optical imaging (OI),[4] computed tomography (CT),[5] magnetic resonance imaging (MRI),[6–8] magnetic resonance spectroscopy (MRS),[9] positron-emission tomography (PET),[10] single photon-emission CT (SPECT),[11] ultrasound (US)[12] and so on. However, given the inherent tradeoff between depth of penetration and spatial resolution due to strong optical scattering,[13] the application of real-time *in vivo* OI techniques are limited to either the thin layers of samples like skin or ocular, or the sacrificed spatial resolution.

Photoacoustic imaging (PAI), combining the benefits of high contrast in OI and the great spatial resolution available from US imaging, has been proved to be a promising molecular imaging approach applied in a growing number of clinical applications.[14,15] It relies on the conversion of photo energy into US waves generated by the thermoelastic expansion of tissue in response to the absorption of short laser pulses.[16,17] Since the acoustic waves are scattered much less than photons in the tissue, PAI provides noninvasive images at great depths (up to 7 cm) with improved resolution ($\sim$100 μm).[18,19] Therefore, PAI could be applied in various clinical fields such as primary tumor detection, therapeutic monitoring, molecular characterization of cancer, metastatic lymph nodes assessment, etc.[14,20–25] As the fastest-growing molecular imaging technique, many efforts have been made to improve the PAI technologies to achieve better resolution and sensitivity over the past two decades,[26–30] especially with various PA probes being extensively developed for high contrast images.[31–33] The ideal PA probes need to exhibit the characteristics such as with strong absorption in the near-infrared optical window, high specificity and stability *in vivo*, good targeting and biocompatibility, easy labeling, low fluorescence quantum yield, no need for exogenous substances, etc. Although a wide range of exogenous contrast agents are available for PAI, such as small-molecule dyes, metallic or semiconducting nanoprobes and organic nanoprobes, their applications *in vivo* are often eliminated by poor specificity and low systemic delivery efficiency.[34] To overcome those limitations, the reporter genes (RGs), which could genetically encode PA contrasts, have been developed to facilitate deep-tissue PAI of the internal tissues and organs by obtaining better resolution at depths previously not achievable by other probes.[35]

RGs have been originally developed in the 1980s, referring to the exogenous DNA segments whose expression products could produce signals that can

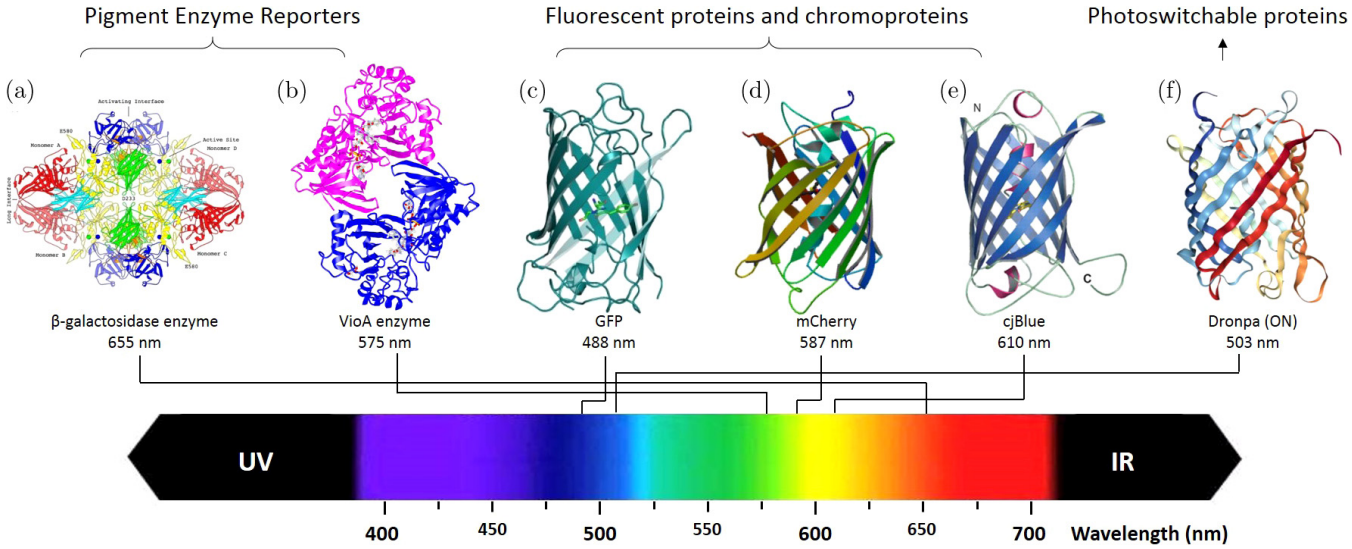

Fig. 1. Crystal structure and absorption maxima of the representative genetic reporters used in PAI. (a) The tetrameric structure of β-galactosidase.[43] (b) Crystal structure of VioA from *C. violaceum*.[44] (c) Crystal structure of Green fluorescent protein (GFP).[45] (d) Crystal structure of mCherry.[46] (e) The monomeric cjBlue subunit.[47] (f) Bright-state structure of the reversibly switchable fluorescent protein Dronpa.[48]

be easily visualized using imaging or chemical analysis.[36] The expression products of RGs, including, for example enzymes, receptors, transporters and metalloproteins, etc. have broad applications for observing molecules of interest.[37] Based on detection of the location and quantification of these products introduced at the cellular, tissue and whole-body levels, specific biological information of organisms could be reflected *in vivo*, facilitating the monitoring of gene therapy, endogenous molecular events, drugs screening, cell implant therapy, and theranostics.[38,39] Moreover, PAI RGs have received considerable attention owing to the attractive strong PA contrast induced by the genetic expression of RGs which could be easily engineered to sense various signaling molecules.[38,40,41] According to the different optical properties of the expression products, current PAI GRs could be classified into three main classes[42]: (1) Pigment enzyme reporters; (2) Fluorescent proteins (FPs) and chromoproteins (CPs); (3) Photoswitchable proteins. In this review, we summarize the PA RGs that have been applied to noninvasive molecular imaging and theranostics (Fig. 1). Emphasis is given on the preclinical results of recent studies. Finally, we discuss the outlook and possible directions for the future studies in PAI RGs.

2. Pigment Enzyme Reporters

Mammalian cells without naturally contained pigments could become light absorbers by introducing the pigment-producing enzymes, exhibiting relatively strong PA signals in living cells. Four enzymatically generated reporters in PAI are discussed in this section: (1) bacterial *LacZ*, which produces a blue pigment with the injection of exogenous X-gal as substrate; (2) human *tyrosinase* (Tyr), which enzymatically generates a brown pigment via the conversion of endogenous tyrosine into melanin; (3) bacterial *violacein*, a violet pigment produced from the sole precursor tryptophan through multienzymes-based oxidation pathway; and (4) human *organic anion-transporting polypeptide 1b3* (*Oatp1b3*).

2.1. *LacZ*

Originating from *Coli*, *LacZ* is a bacterial gene which encodes β-galactosidase.[49] In the presence of the metabolic enzymes β-galactosidase, a blue pigment product (5,5′-dibromo-4,4′-dichloroindigo) with a strong absorption between 600 and 700 nm could be yield as a contrast agent for PAI. However, the pigment formation requires the injection of exogenous X-gal (5-bromo-4-chloro-3-indolyl-β-D-galactoside) as substrate, which is a colorless analogue of lactose that may causes occasional skin irritation and inflammation in addition to the inefficient delivery and metabolism *in vivo*. Via applying *LacZ* in PAI, Wang and colleagues[50] obtained the detailed *in vivo* morphology of gliosarcoma tumor cells and its surrounding microvasculature simultaneously. Subsequently, they visualized *LacZ* in a subcutaneous tumor at the depth of 5.0 cm with lateral and axial resolutions of ∼1.0 and ∼0.4 mm, respectively,[51] suggesting the feasibility of using *LacZ* as a RG in PAI *in vivo*.

2.2. *Tyrosinase*

As the most widely applied enzymatic reporter for generating PA contrast, Tyr is the primary enzyme responsible for melanin production in melanogenic tissues.[52–54] It converts the amino acid tyrosine to the brown melanin pigment as strong absorption contrast agents for PAI, and thus has been validated as a dual RG for PAI by introducing into nonmelanogenic cells.[54] Unlike β-galactosidase, there is no requirement of exogenous substrate for producing melanin from tyrosine in the nonmelanogenic cells. Instead, it is the endogenous and ubiquitous tyrosine in cells that are utilized by Tyr as the substrates to produce the pigment.[54] Moreover, the melanin pigments exhibit a broad absorption spectrum even extending to the near-infrared, making it a more suitable reporter for *in vivo* PAI.[55]

For example, by introducing Tyr, Gillanders *et al.*[56] demonstrated that the signal from transfected cells was increased by more than 10 times over wild-type cells, confirming the efficacy of using Tyr as the PAI RG *in vivo*. Subsequently, a system of inducible Tyr RP expression triggered by doxycycline in xenograft tumors was developed by Paproski *et al.*[57] providing a powerful tool for obtaining strong signals for *in vivo* high-resolution multiwavelength tumor PAI. Furthermore, to improve the imaging contrast and maintain the visualization of Tyr-expressing cells in different generations, Jathoul *et al.*[55] took advantages of stable

retroviral transduction and developed a new deep-tissue PAI system, achieving the monitoring of tumor growth over a long time period up to 52 days. However, Tyr is barely expressed in bacterial, causing the limitation on monitoring the bacterial infections or theranostic applications. To overcome this problem, Paproski *et al.*[58] found the bacterial Tyr homologue *melA*, which could be a promising candidate as bacterial photoacoustic RG with strong fluorescence and luciferase activity.

Although with several advantages, the over-expression of Tyr would be harmful to cells with long persistence time and other toxic effects, like skin aging, Pakinson's disease and melanoma and so on.[59,60] Therefore, the expression level of Tyr should be critically controlled in order to minimize the potential cytotoxicity.

2.3. *Violacine*

Undergoing the genetically controlled biosynthesis involving five *Chromobacterium violaceum* enzymes (*Vio*A, *Vio*B, *Vio*C, *Vio*D, and *Vio*E),[61] the deep-purple pigment violacein, which is a bacterial quorum-sensing chromophore, could be enzymatically generated from the *L*-tryptophan.[62] The synthesized violacein could serve as a bacterial label for *in vivo* PAI in the near-infrared with high photobleaching resistance. Although Jiang *et al.* further demonstrated anti-cancer activity of violacein *in vitro*, so far violacein has only been expressed in bacteria, unlike *lacZ* and Tyr with mammalian cells application. Though being primarily considered as an environmental organism, the involvement of *C. violaceum* as a pathogen in human infections have been reported,[63,64] making the possibility of its theranostic application still need to be explored.[65]

2.4. *Organic anion-transporting polypeptide 1b3 (OATP1B3)*

The human organic anion-transporting polypeptides (OATPs) refer to 12 transmembrane glycoproteins involved in the cellular uptake of small anion molecules in liver and intestine,[66] OATP1B1 and OATP1B3 of which were initially developed as MRI contrast agent.[67] Recently, Wu *et al.*[68] demonstrated the feasibility of using indocyanine green (ICG) fluorescence imaging facilitated by OATP1B3 as an *in vivo* strategy for noninvasive imaging a HT-1080 tumor-bearing nude mouse with high specificity and long observation period up to 96 h, expanding its potential applications in oncology, cell transplantation, and tissue engineering.[69,70]

Although these enzymatic RGs could offer benefits of the inherent signal amplification of the genetic signal with potentially higher local concentrations, the dependence on availability of the substrate would hinder the accurate interpretation of assay which relying largely on quantifications of gene expression. Additionally, their unambiguous detection *in vivo* and in deep tissue remains challenging due to the low absorption coefficient.

3. FPs and CPs

In addition to the enzymatic reporters, several nonenzymatic reporters have been studied for PAI as well, including fluorescent or nonfluorescent reporters. Due to their robust photostability and high photoacoustic generation efficiency, the nonenzymatic reporters become more appreciated. Another advantage of the nonenzymatic reporters is the 1:1 mapping between the detected protein and the RG expression, allowing for the quantitate studies. As differentiated by the optical properties, three classes of nonenzymatic reporters are discussed in this section: (1) autofluorescent proteins (AFPs), (2) nonfluorescent proteins (Chromoproteins, CPs), and (3) Bacterial photochrome photoreceptors (BphPs).

3.1. *Autofluorescent GFP and GFP-like proteins*

As a typical AFPs, GFP, which was naturally originated from jellyfish and has been widely applied as fluorescent markers in biomedical studies.[71] Subsequently, with a common structure consisting of β-barrel scaffold containing the chromophore as GFP, more GFP-like AFPs have been isolated from other marine organisms such as sea anemones and corals. Since the autofluorescence formed by folding of the polypeptide chain with absence of any substrates or cofactors, the nontoxic AFPs are more preferable in molecular imaging in living cells and organisms.[72]

In 2009, Razansky *et al.*[73] published the first study of successfully applying GFP and mCherry in PAI of fruit fly pupae and adult zebrafish.

Comparing with fluorescence, they obtained higher spatial resolution and deeper penetrations. However, their relatively high quantum yields (QYs) and low absorption in NIR region limited the application in more organisms. Compared to GFP and mCherry, far-red FPs with red-shifted absorption spectra and lower QYs were supposed to provide stronger signals for PAI *in vivo*.[74,75] However, because of the photobleaching and fluorescence emission problems, the photostability of far-red FPs still needs to be improved.

More GFP and GFP-like AFPs, such as dsRed,[76] mNeptune,[77] mRaspberry,[78] E2 Crimson,[79] etc. have been widely applied as well. Despite the successful attempts in the visualization of cells in comparatively small and transparent organisms[73,80] and in xenografts in small mammals,[81] it is still challenging for FPs to eliminate the reduced PA contrast at comparatively low fluences compared to nonfluorescent absorbers due to photobleaching and ground state depopulation.[74]

3.2. *Chromoproteins*

The coral reefs are colored by not only FPs but also CPs, both of which constitute homologous to GFP.[82,83] The nonfluorescent GFP-like proteins with the absorption of orange-red light, referring as CPs, were developed to address the challenges of photobleaching and efficiency of PA signal generation in AFPs.[84] Comparing with FPs and enzyme reporters, there are certain advantages of CPs, such as efficient Förster resonance energy transfer quenching, instrument-free detection, and absence of exogenous substrate, making CPs more attractive as RGs for PAI.[85]

For example, the CPs (e.g., aeCP597 Refs. 78 and 86, cjBlue Ref. 47, and E2-Crimson NF Ref. 74) that initially applied in the *in vitro* measurement of PA spectrum and photobleaching exhibited significantly higher photoacoustic generation efficiency and photostability compared to the FPs, mainly due to the absence of radiative relaxation and ground state depopulation.[74] Moreover, several improved CPs variants were developed and significant enhancements in PA signals were obtained.[47,87]

Recently, Forster *et al.*[85] tested the availability of 14 engineered CP genes (such as meffRed, scOrange, amilGFP, gfasPurple and so on) in *coli*. The *in vivo* imaging demonstrated the potential of using integrating pairs or engineering version of CPs for providing genetically encoded PA contrast.

Using CPs as the RGs in PAI exhibited greater photoacoustic signal generation efficiency since they are not susceptible to photobleaching, suggesting the potential of CPs in providing genetically encoded PA contrast. However, they have not yet been expressed efficiently in mammalian cells, which still need to be explored for *in vivo* applications.

3.3. *Bacterial phytochrome photoreceptors (BphPs)*

Phytochrome, originated from plants, fungi, bacterial and cyanobacteria, are light-sensitive proteins with different types of tetrapyrroles as chromophores.[40] BphPs refer to the bacterial photoreceptors associated with the chromophore of endogenous biliverdin (BV), which is a heme-derived tetrapyrrole available in mammalian tissues. The deduced autofluorescence and low light scattering of the endogenous chromophores make BphPs more suitable to deep tissue PAI.[88] Since mammalian tissue is relatively transparent to NIR light, in recent years, several NIR FPs have been developed from BphPs as a subset in the NIR window with the spectral region from 650 nm to 900 nm.[89,90] Comparing with GFP-like FPs, the deep penetration of NIR light in tissue makes NIR FPs superior for deep-tissue *in vivo* PAI, with lower fluorescence QY (~6%) and higher intrinsic extinction coefficient (~100 m $M^{-1}cm^{-1}$, for GFP-like proteins are ~60% and ~56 m $M^{-1}cm^{-1}$, respectively). NIR BphPs can convert between two different photochemical states, from red absorbing (Pr) to far-red absorbing (Pfr) state and *vice versa*.

Currently, there are about 20 different NIR BphPs applied *in vivo* and live-cell, such as the iRFPs,[26,91] infrared fluorescent proteins[92] and mIFP,[93] miRFPs,[94] AphB,[95] Wi-Phy[96] and so on.[97] The NIR BphP was developed in 2012 by Filonov and colleges,[26] who compared the performance of a near-infrared fluorescent protein (iRFP) with several far-red-shifted GFP-like FPs in deep-tissue photoacoustic tomography, and demonstrated iRFP713, derived from the domain of the photosynthetic bacterium *Rhodopseudomonas palustris* (*Rp*BphP2) as template, as a promising probe for noninvasive tumor monitoring based on the stronger photoacoustic signals (2.2-fold increase) and

better resolution (280 μm lateral and 75 μm axial) at the depth of 4 mm obtained under 680 nm in live animal. Subsequently, Shcherbakova and Verkhusha[91] reported four BphP-based NIR FPs, such as iRFP670, iRFP682, iRFP702 derived from *Rp*BphP6 and iRFP720 engineered from *Rp*BphP2, which showed high effective brightness and low cytotoxicity in mammalian cells and mice, allowing multicolor NIR imaging *in vivo*. However, despite the NIR BphPs developed from *Rp*BphP2 and *Rp*BphP6 could be applied in whole-cell imaging, the limitation of the dimeric NIR FPs in the application as protein fusion tags cannot be neglected since their oligomeric state might affect the functionality of target proteins.[88] Therefore, monomeric versions of infrared fluorescent proteins were developed by Yu *et al.*[92] in 2014 and the better imaging capabilities of the developed IFP1.4 and IFP2.0 in *Drosophila* larvae and whole mice were demonstrated. However, both of them tend to dimerize at high concentration. To overcome this problem, in the following year, they developed the robust naturally monomeric IFP (mIFP) which could correctly label proteins in live cells, *Drosophila* and zebrafish,[93] but a supply of BV via co-expression of BV-producing enzyme were required. Furthermore, three bright spectrally distinct monomeric NIR FPs (miRFPs) were reported, which showed 2–5-fold brighter in mammalian cells than previous NIR FPs, thus allow noninvasive visualization and detection of biological processes at different scales.[94] Other NIR FPs developed from the domains of the bacteriophytochrome like AphB, *Dr*BphP and *Dr*BphP-PCM hold great potential for noninvasive deep-tissue functional imaging.[89,95,96,98,99]

Owing to the substantially red-shifted absorption spectra and high extinction coefficient, the bacteriophytochrome-derived fluorescent probes are less susceptible to photobleaching and exhibit significantly higher penetration depth and PA contrast than conventional GFP-like proteins. However, the injection of cofactors or multienzymes are typically required to generate the imaging signals, except for mammals.

4. Reversibly Photoswitchable Proteins (rPSPs)

The recent emerged rPSPs are another kind of nonenzymatic reporters, the protein isomeric states of which could be selectively and reversibly switched between ON to OFF with distinct absorption peaks at the same wavelength exhibited. Such a unique contrast mechanisms of rPSPs make them useful for high-contrast PAI because of the eliminated background contrast and the enhanced detection specificity and sensitivity.[100] Increasing number of researchers have explored the capability of several fluorescent rPSPs (Dronpa, reTagRFP) and nonfluorescent rPSPs (BphP1, AGP1).

For example, among the different rPSPs, most of the transgene imaging labels for PAI are the GFP-like AFPs derived from corals, such as the proteins of Dronpa and its fast-switching fatigue-resistant variant Dronpa-M159T,[101] which were shown to be high-contrast PA gene reporters for *in vivo* imaging and bacterial tumor tracking. For another example, as the first monomeric red FP of rPSPs, rsTagRFP can be switched between red fluorescent state (ON) and nonfluorescent state (OFF) with the photoswitchable absorbance spectra at 567 and 440 nm, induced by yellow and blue light, respectively.[102,103] Thus, rsTagRFP can be used as a photochromic acceptor for protein–protein interaction *in vivo*, especially for the photochromic Förster resonance energy transfer (pcFRET).

Moreover, the reversibly switching of the nonfluorescent rPSPs *Rp*BphP1 between Pfr (ON) and Pr (OFF) states was successfully applied by Yao *et al.*[104] in diagnosis of BphP1-expressing tumors and monitoring the metastases with improved resolution and higher contrast. However, in addition to the complexity and cost of this two-dimensional (2D) imaging approach, the photoswitching-induce absorption changes at other wavelengths were not exploited. To overcome these disadvantages, a recent study reported a methodology of dual-wavelength three-dimensional (3D) *in vivo* PA RG imaging of tumors in deep tissue, which was based on the use of phytochrome AGP1 as a imaging reporter protein and dual wavelength signal acquisition.[105] Given the experimental simplicity and ease of implementation of this approach, it is highly attractive for RG imaging for longitudinal preclinical study.

With the reversibly photoswitching capabilities between red and NIR absorption states, rPSPs could significantly improve the imaging contrast, remove the background contrast, enhance the spatial resolution and eliminate the photobleaching

effect, making them more suitable for PAI imaging at NIR absorption for deep tissues.

5. Outlook

PAI has potentially great impact on biomedical research as well as clinical practice over these decades. With the different technologies developed for PAI these years, the detection limits of noninvasive molecular imaging have been pushed further, enabling us to fulfil the requirements of high-resolution *in vivo* images in deep tissue for biomedical studies. When combined with proper RGs as genetically encoded probes for the noninvasive molecular imaging, PAI becomes more powerful in obtaining higher spatial resolution with improved penetration depths, showing great advantages for the basic researches and preclinical and clinical applications, such as the complex biological processes of gene expression, tumor growth, cell distribution, molecular interaction, intracellular signaling, differentiation and so on.[106] Moreover, PAI RGs also have the potentials to be developed to modulate neuronal activities in deep brain with high resolution in the future.[107,108] Among the various existing RGs for PAI, rPSPs show the most remarkable performance as the reporter candidates for deep tissue *in vivo* PAI, given the improved imaging contrast and the removal of endogenous background signals due to the reversible photoswitching properties. Further works could focus on engineering the rPSPs-based biosensors in order to obtain greater applicability for deep-tissue imaging *in vivo*.

Although increasing number of RGs has been developed for PAI in recent years with broad applications in laboratory and clinical performances, the clinical translation of PAI RGs in theranostics remains challenging with more work needed to further improve this technology in the following aspects. First, the detection sensitivity still needs to be improved by engineering RGs with more favorable absorption characteristics and more efficient protein expression in PAI. Second, the spatiotemporal precision and quantification of PAI RGs must be developed by the technical improvements in the hardware and software, and in the spectral unmixing model establishment in PAI, which could reveal the expression or migration patterns of target moleculars in deep tissue. Third, to obtain more complementary and informative observation of the deep tissue *in vivo*, RGs that could be applied in the integration of PAI with other imaging techniques like fluorescence or US imaging should be further developed. Finally, the safety issues of certain RGs with the requirement of introducing exogenous genetic materials still need to be considered. We believe that with the continuous improvements of the PAI RGs, more clinical studies could be explored to exhibit the potential of this imaging technology in theranostics and other biomedical fields.

Acknowledgments

This work was supported by the Major State Basic Research Development Program of China (2017YFA0205201 and 2018YFA0107301), the National Natural Science Foundation of China (81422023, 81925019, 81603015, 81801817, U1705281, and U1505221), the Fundamental Research Funds for the Central Universities (20720190088), Natural Science Foundation of Fujian Province (2016J05202 and JT180649), and the Program for New Century Excellent Talents in University, China (NCET-13-0502).

References

1. T. F. Massoud, S. S. Gambhir, "Molecular imaging in living subjects: Seeing fundamental biological processes in a new light," *Genes Dev.* **17**(5), 545–580 (2003).
2. T. F. Massoud, S. S. Gambhir, "Integrating noninvasive molecular imaging into molecular medicine: An evolving paradigm," *Trends Mol. Med.* **13**(5), 183–191 (2007).
3. Z. Lei *et al.*, "Biomimetic synthesis of nanovesicles for targeted drug delivery," *Sci. Bull.* **63**(11), 663–665 (2018).
4. V. Ntziachristos, "Going deeper than microscopy: The optical imaging frontier in biology," *Nat. Methods* **7**(8), 603 (2010).
5. D. J. Brenner, E. J. Hall, "Computed tomography — an increasing source of radiation exposure," *New England J. Med.* **357**(22), 2277–2284 (2007).
6. S. A. Huettel, A. W. Song, G. McCarthy, *Functional Magnetic Resonance Imaging*, Vol. 1, Sinauer Associates Sunderland, MA (2004).
7. C. Yang *et al.*, "Metalla-aromatic loaded magnetic nanoparticles for MRI/photoacoustic imaging-guided cancer phototherapy," *J. Mater. Chem. B* **6**(17), 2528–2535 (2018).

8. X. Wang *et al.*, "Gadolinium embedded iron oxide nanoclusters as T 1–T 2 dual-modal MRI-visible vectors for safe and efficient siRNA delivery," *Nanoscale* **5**(17), 8098–8104 (2013).
9. J. W. Emsley, J. Feeney, L. H. Sutcliffe, *High Resolution Nuclear Magnetic Resonance Spectroscopy*, Vol. 2, Elsevier (2013).
10. S. S. Gambhir, "Molecular imaging of cancer with positron emission tomography," *Nat. Rev. Cancer* **2**(9), 683 (2002).
11. K. Ogawa *et al.*, "A practical method for position-dependent Compton-scatter correction in single photon emission CT," *IEEE Trans. Med. Imag.* **10**(3), 408–412 (1991).
12. J.-U. Voigt, "Ultrasound molecular imaging," *Methods* **48**(2), 92–97 (2009).
13. C. Errico *et al.*, "Ultrafast ultrasound localization microscopy for deep super-resolution vascular imaging," *Nature* **527**(7579), 499 (2015).
14. C. Li, L. V. Wang, "Photoacoustic tomography and sensing in biomedicine," *Phys. Med. Biol.* **54**(19), R59 (2009).
15. M. Xu, L. V. Wang, "Photoacoustic imaging in biomedicine," *Rev. Sci. Instrum.* **77**(4), 041101 (2006).
16. D. Grootendorst *et al.*, "First experiences of photoacoustic imaging for detection of melanoma metastases in resected human lymph nodes," *Lasers Surg. Med.* **44**(7), 541–549 (2012).
17. S. Wang *et al.*, "Recent advances in photoacoustic imaging for deep-tissue biomedical applications," *Theranostics* **6**(13), 2394 (2016).
18. L. V. Wang, S. Hu, "Photoacoustic tomography: In vivo imaging from organelles to organs," *Science* **335**(6075), 1458–1462 (2012).
19. J. Yao, L. Song, L. V. Wang, "Photoacoustic microscopy: Superdepth, superresolution, and superb contrast," *IEEE Pulse* **6**(3), 34–37 (2015).
20. D. Razansky *et al.*, "Deep tissue optical and optoacoustic molecular imaging technologies for pre-clinical research and drug discovery," *Current Pharm. Biotechnol.* **13**(4), 504–522 (2012).
21. Y. Liu, L. Nie, X. Chen, "Photoacoustic molecular imaging: From multiscale biomedical applications towards early-stage theranostics," *Trends Biotechnol.* **34**(5), 420–433 (2016).
22. R. M. Weight, P. S. Dale, J. A. Viator, Detection of circulating melanoma cells in human blood using photoacoustic flowmetry, *2009 Annual Int. Conf. IEEE Engineering in Medicine and Biology Society*, IEEE (2009).
23. E. Ren *et al.*, "Magnetosome modification: From bio-nano engineering toward nanomedicine," *Adv. Therapeutics* **1**(6), 1800080 (2018).
24. M. Chen *et al.*, "Safety profile of two-dimensional Pd nanosheets for photothermal therapy and photoacoustic imaging," *Nano Res.* **10**(4), 1234–1248 (2017).
25. L. Li, X. Pang, G. Liu, "Near-infrared light-triggered polymeric nanomicelles for cancer therapy and imaging," *ACS Biomater. Sci. Eng.* **4**(6), 1928–1941 (2017).
26. G. S. Filonov *et al.*, "Deep-tissue photoacoustic tomography of a genetically encoded near-infrared fluorescent probe," *Angew. Chem. Int. Ed.* **51**(6), 1448–1451 (2012).
27. J. Zhang *et al.*, "Biocompatible D–A semiconducting polymer nanoparticle with Light-harvesting unit for highly effective photoacoustic imaging guided photothermal therapy," *Adv. Funct. Mater.* **27**(13), 1605094 (2017).
28. X. R. Song *et al.*, "Co9Se8 nanoplates as a new theranostic platform for photoacoustic/magnetic resonance dual-modal-imaging-guided chemo-photothermal combination therapy," *Adv. Mater.* **27**(21), 3285–3291 (2015).
29. J. Ye *et al.*, "Noninvasive magnetic resonance/photoacoustic imaging for photothermal therapy response monitoring," *Nanoscale* **10**(13), 5864–5868 (2018).
30. X. Wang *et al.*, "Size-controlled biocompatible silver nanoplates for contrast-enhanced intravital photoacoustic mapping of tumor vasculature," *J. Biomed. Nanotechnol.* **14**(8), 1448–1457 (2018).
31. Q. Fu *et al.*, "Photoacoustic imaging: Contrast agents and their biomedical applications," *Adv. Mater.* **31**(6), 1805875 (2019).
32. L. V. Wang, "Prospects of photoacoustic tomography," *Med. Phys.* **35**(12), 5758–5767 (2008).
33. M. Chen *et al.*, "Core–shell Pd@Au nanoplates as theranostic agents for in-vivo photoacoustic imaging, CT imaging, and photothermal therapy," *Adv. Mater.* **26**(48), 8210–8216 (2014).
34. J. Yao, L. V. Wang, "Recent progress in photoacoustic molecular imaging," *Curr. Opin. Chem. Biol.* **45**, 104–112 (2018).
35. J. H. Kang, J.-K. Chung, "Molecular-genetic imaging based on reporter gene expression," *J. Nucl. Med.* **49**, 164S (2008).
36. P. Ray, A. De, "Reporter gene imaging in therapy and diagnosis," *Theranostics* **2**(4), 333 (2012).
37. P. Brader, I. Serganova, R. G. Blasberg, "Noninvasive molecular imaging using reporter genes," *J. Nucl. Med.* **54**(2), 167–172 (2013).
38. C. Liu *et al.*, "Advances in imaging techniques and genetically encoded probes for photoacoustic imaging," *Theranostics* **6**(13), 2414–2430 (2016).

39. L. Cheng *et al.*, "PEGylated Prussian blue nanocubes as a theranostic agent for simultaneous cancer imaging and photothermal therapy," *Biomaterials* **35**(37), 9844–9852 (2014).
40. K. Mishra *et al.*, *Photocontrollable Proteins for Optoacoustic Imaging*, ACS Publications (2019).
41. J. Brunker *et al.*, "Photoacoustic imaging using genetically encoded reporters: A review," *J. Biomed. Opt.* **22**(7), 070901 (2017).
42. D. M. Shcherbakova *et al.*, "Natural photoreceptors as a source of fluorescent proteins, biosensors, and optogenetic tools," *Ann. Rev. Biochem.* **84**, 519–550 (2015).
43. D. H. Juers, B. W. Matthews, R. E. Huber, "LacZ β-galactosidase: Structure and function of an enzyme of historical and molecular biological importance," *Protein Sci.* **21**(12), 1792–1807 (2012).
44. J. J. Füller *et al.*, "Biosynthesis of violacein, structure and function of l-Tryptophan oxidase VioA from Chromobacterium violaceum," *J. Biol. Chem.* **291**(38), 20068–20084 (2016).
45. M. Ormö *et al.*, "Crystal structure of the Aequorea victoria green fluorescent protein," *Science* **273** (5280), 1392–1395 (1996).
46. X. Shu *et al.*, "Novel chromophores and buried charges control color in mFruits," *Biochemistry* **45**(32), 9639–9647 (2006).
47. M. C. Chan *et al.*, "Structural characterization of a blue chromoprotein and its yellow mutant from the sea anemone Cnidopus japonicus," *J. Biol. Chem.* **281**(49), 37813–37819 (2006).
48. A. C. Stiel *et al.*, "1.8 Å bright-state structure of the reversibly switchable fluorescent protein Dronpa guides the generation of fast switching variants," *Biochem. J.* **402**(1), 35–42 (2007).
49. L. Li *et al.*, "Photoacoustic imaging of lacZ gene expression in vivo," *J. Biomed. Opt.* **12**(2), 020504 (2007).
50. L. Li *et al.*, "Simultaneous imaging of a lacZ-marked tumor and microvasculature morphology in vivo by dual-wavelength photoacoustic microscopy," *J. Innov. Opt. Health Sci.* **1**(2), 207–215 (2008).
51. X. Cai *et al.*, "Multi-scale molecular photoacoustic tomography of gene expression," *PLoS One* **7**(8), e43999 (2012).
52. V. Del Marmol, F. Beermann, "Tyrosinase and related proteins in mammalian pigmentation," *FEBS Lett.* **381**(3), 165–168 (1996).
53. H. Zheng *et al.*, "Tyrosinase-based Reporter gene for photoacoustic imaging of MicroRNA-9 regulated by DNA methylation in living subjects," *Mol. Ther. Nucleic Acids* **11**, 34–40 (2018).
54. R. J. Paproski *et al.*, "Tyrosinase as a dual reporter gene for both photoacoustic and magnetic resonance imaging," *Biomed. Opt. Exp.* **2**(4), 771–780 (2011).
55. A. P. Jathoul *et al.*, "Deep in vivo photoacoustic imaging of mammalian tissues using a tyrosinase-based genetic reporter," *Nat. Photonics* **9**(4), 239 (2015).
56. A. Krumholz *et al.*, "Photoacoustic microscopy of tyrosinase reporter gene in vivo," *J. Biomed. Opt.* **16**(8), 080503 (2011).
57. R. J. Paproski *et al.*, "Multi-wavelength photoacoustic imaging of inducible tyrosinase reporter gene expression in xenograft tumors," *Sci. Rep.* **4**, 5329 (2014).
58. R. J. Paproski *et al.*, "Validating tyrosinase homologue melA as a photoacoustic reporter gene for imaging Escherichia coli," *J. Biomed. Opt.* **20**(10), 106008 (2015).
59. X. Li, "Gelatinase inhibitors: A patent review (2011–2017)," *Expert Opin. Ther. Pat.* **28**(1), 31–46 (2018).
60. A. Bose, G. A. Petsko, D. Eliezer, "Parkinson's disease and melanoma: Co-occurrence and mechanisms," *J. Parkinson's Disease* **8**(3), 385–398 (2018).
61. N. Durán *et al.*, "Advances in Chromobacterium violaceum and properties of violacein-Its main secondary metabolite: A review," *Biotechnol. Adv.* **34**(5), 1030–1045 (2016).
62. Y. Jiang *et al.*, "Violacein as a genetically-controlled, enzymatically amplified and photobleaching-resistant chromophore for optoacoustic bacterial imaging," *Sci. Rep.* **5**, 11048 (2015).
63. A. Chattopadhyay *et al.*, "Chromobacterium violaceum infection: A rare but frequently fatal disease," *J. Pediatric Surg.* **37**(1), 108–110 (2002).
64. E. Bottieau *et al.*, "Fatal Chromobacterium violaceum bacteraemia in rural Bandundu, Democratic Republic of the Congo," *New Microbes New. Infect.* **3**, 21–23 (2015).
65. V. Kothari, S. Sharma, D. Padia, "Recent research advances on Chromobacterium violaceum," *Asian Pacific J. Tropical Med.* **10**(8), 744–752 (2017).
66. M. Svoboda *et al.*, "Organic anion transporting polypeptides (OATPs): Regulation of expression and function," *Curr. Drug Metabolism* **12**(2), 139–153 (2011).
67. M. Leonhardt *et al.*, "Hepatic uptake of the magnetic resonance imaging contrast agent Gd-EOB-DTPA: Role of human organic anion transporters," *Drug Metab. Dispos.* **38**(7), 1024–1028 (2010).
68. M.-R. Wu *et al.*, "Organic anion-transporting polypeptide 1B3 as a dual reporter gene for

fluorescence and magnetic resonance imaging," *FASEB J.* **32**(3), 1705–1715 (2017).
69. M. Li *et al.*, "Multimodality reporter gene imaging: Construction strategies and application," *Theranostics* **8**(11), 2954 (2018).
70. M.-R. Wu, Y.-Y. Huang, J.-K. Hsiao, "Use of indocyanine green (ICG), a medical near infrared dye, for enhanced fluorescent imaging — comparison of organic anion transporting polypeptide 1B3 (OATP1B3) and sodium-taurocholate cotransporting polypeptide (NTCP) reporter genes," *Molecules* **24**(12), 2295 (2019).
71. T. Drepper *et al.*, "Reporter proteins for *in vivo* fluorescence without oxygen," *Nat. Biotechnol.* **25**(4), 443 (2007).
72. A. S. Mishin *et al.*, "Novel uses of fluorescent proteins," *Curr. Opin. Chem. Biol.* **27**, 1–9 (2015).
73. D. Razansky *et al.*, "Multispectral opto-acoustic tomography of deep-seated fluorescent proteins in vivo," *Nat. Photonics* **3**(7), 412 (2009).
74. J. Laufer *et al.*, "In vitro characterization of genetically expressed absorbing proteins using photoacoustic spectroscopy," *Biomed. Opt. Exp.* **4**(11), 2477–2490 (2013).
75. N. C. Deliolanis *et al.*, "Deep-tissue reporter-gene imaging with fluorescence and optoacoustic tomography: A performance overview," *Mol. Imag. Biol.* **16**(5), 652–660 (2014).
76. B. J. Bevis, B. S. Glick, "Rapidly maturing variants of the Discosoma red fluorescent protein (DsRed)," *Nat. Biotechnol.* **20**(1), 83 (2002).
77. M. Z. Lin *et al.*, "Autofluorescent proteins with excitation in the optical window for intravital imaging in mammals," *Chem. Biol.* **16**(11), 1169–1179 (2009).
78. L. Wang *et al.*, "Evolution of new nonantibody proteins via iterative somatic hypermutation," *Proc. Natl. Acad. Sci.* **101**(48), 16745–16749 (2004).
79. R. L. Strack *et al.*, "A rapidly maturing far-red derivative of DsRed-Express2 for whole-cell labeling," *Biochemistry* **48**(35), 8279–8281 (2009).
80. M. Liu *et al.*, "In vivo three dimensional dual wavelength photoacoustic tomography imaging of the far red fluorescent protein E2-Crimson expressed in adult zebrafish," *Biomed. Opt. Exp.* **4**(10), 1846–1855 (2013).
81. A. Krumholz *et al.*, "Multicontrast photoacoustic in vivo imaging using near-infrared fluorescent proteins," *Sci. Rep.* **4**, 3939 (2014).
82. N. O. Alieva *et al.*, "Diversity and evolution of coral fluorescent proteins," *PLoS One* **3**(7), e2680 (2008).
83. D. M. Shcherbakova, V. V. Verkhusha, "Chromophore chemistry of fluorescent proteins controlled by light," *Curr. Opin. Chem. Biol.* **20**, 60–68 (2014).
84. P. Dedecker, F. C. De Schryver, J. Hofkens, "Fluorescent proteins: Shine on, you crazy diamond," *J. Amer. Chem. Soc.* **135**(7), 2387–2402 (2013).
85. J. Liljeruhm *et al.*, "Engineering a palette of eukaryotic chromoproteins for bacterial synthetic biology," *J. Biol. Eng.* **12**(1), 8 (2018).
86. M. A. Shkrob *et al.*, "Far-red fluorescent proteins evolved from a blue chromoprotein from Actinia equina," *Biochem. J.* **392**(3), 649–654 (2005).
87. A. Pettikiriarachchi *et al.*, "Ultramarine, a chromoprotein acceptor for Förster resonance energy transfer," *PloS One* **7**(7), e41028 (2012).
88. G. Gourinchas, S. Etzl, A. Winkler, "Bacteriophytochromes–from informative model systems of phytochrome function to powerful tools in cell biology," *Curr. Opin. Struct. Biol.* **57**, 72–83 (2019).
89. K. G. Chernov *et al.*, "Near-infrared fluorescent proteins, biosensors, and optogenetic tools engineered from phytochromes," *Chem. Rev.* **117**(9), 6423–6446 (2017).
90. M. Karasev *et al.*, "Near-Infrared Fluorescent Proteins and Their Applications," *Biochemistry (Moscow)* **84**(1), 32–50 (2019).
91. D. M. Shcherbakova, V. V. Verkhusha, "Near-infrared fluorescent proteins for multicolor in vivo imaging," *Nat. Methods* **10**(8), 751 (2013).
92. D. Yu *et al.*, "An improved monomeric infrared fluorescent protein for neuronal and tumour brain imaging," *Nat. Commun.* **5**, 3626 (2014).
93. D. Yu *et al.*, "A naturally monomeric infrared fluorescent protein for protein labeling in vivo," *Nat. Methods* **12**(8), 763 (2015).
94. D. M. Shcherbakova *et al.*, "Bright monomeric near-infrared fluorescent proteins as tags and biosensors for multiscale imaging," *Nat. Commun.* **7**, 12405 (2016).
95. C. Yuan *et al.*, "Near infrared fluorescent biliproteins generated from bacteriophytochrome AphB of Nostoc sp. PCC 7120," *Photochem. Photobiol. Sci.* **15**(4), 546–553 (2016).
96. M. E. Auldridge *et al.*, "Structure-guided engineering enhances a phytochrome-based infrared fluorescent protein," *J. Biol. Chem.* **287**(10), 7000–7009 (2012).
97. D. M. Shcherbakova *et al.*, "Near-infrared fluorescent proteins: Multiplexing and optogenetics across scales," *Trends Biotechnol.* **36**(12), 1230–1243 (2018).
98. L. Li *et al.*, "Small near-infrared photochromic protein for photoacoustic multi-contrast imaging

and detection of protein interactions in vivo," *Nat. Commun.* **9**(1), 2734 (2018).

99. L. Li *et al.*, *In vivo photoacoustic multi-contrast imaging and detection of protein interactions using a small near-infrared photochromic protein*, *Photons Plus Ultrasound: Imaging and Sensing 2019*, International Society for Optics and Photonics (2019).
100. P. Vetschera *et al.*, "Characterization of reversibly switchable fluorescent proteins in optoacoustic imaging," *Anal. Chem.* **90**(17), 10527–10535 (2018).
101. A. C. Stiel *et al.*, "High-contrast imaging of reversibly switchable fluorescent proteins via temporally unmixed multispectral optoacoustic tomography," *Opt. Lett.* **40**(3), 367–370 (2015).
102. F. V. Subach *et al.*, "Red fluorescent protein with reversibly photoswitchable absorbance for photochromic FRET," *Chem. Biol.* **17**(7), 745–755 (2010).
103. S. Pletnev *et al.*, "A structural basis for reversible photoswitching of absorbance spectra in red fluorescent protein rsTagRFP," *J. Mol. Biol.* **417**(3), 144–151 (2012).
104. J. Yao *et al.*, "Multiscale photoacoustic tomography using reversibly switchable bacterial phytochrome as a near-infrared photochromic probe," *Nat. Methods* **13**(1), 67 (2016).
105. J. Märk *et al.*, "Dual-wavelength 3D photoacoustic imaging of mammalian cells using a photoswitchable phytochrome reporter protein," *Commun. Phys.* **1**(1), 3 (2018).
106. E. Brown, J. Brunker, S. E. Bohndiek, "Photoacoustic imaging as a tool to probe the tumour microenvironment," *Disease Models Mech.* **12**(7), dmm039636 (2019).
107. J. Yao, L. V. Wang, "Photoacoustic brain imaging: From microscopic to macroscopic scales," *Neurophotonics* **1**(1), 011003 (2014).
108. P. Zhang *et al.*, "High-resolution deep functional imaging of the whole mouse brain by photoacoustic computed tomography in vivo," *J. Biophotonics* **11**(1), e201700024 (2018).